Research article

Computational modeling, analysis and simulation for lockdown dynamics of COVID-19 and domestic violence

Comfort Ohajunwa[1], Carmen Caiseda[2,*]and Padmanabhan Seshaiyer[3]

[1] Governor's School @ Innovation Park, USA

[2] Inter American University of Puerto Rico, Bayamon, USA

[3] George Mason University, USA

* **Correspondence:** Email: ccaiseda@bayamon.inter.edu.

Abstract: As potential strategies to control the spread of COVID-19, governments all across the globe have implemented interventions such as lockdowns and confinement. While these strategies have helped to control the spread, there have also been evidence of widespread increase in Domestic Violence (DV) which is often under-reported. In this work, we have developed two new models that will help study the relationship between lockdowns, the spread of COVID-19 and DV in the hope of mitigating the social problems that follow such drastic measures. Two different models, in increasing level of complexity have been employed to simulate the effect of the lockdown strategy in the spread of COVID-19 and DV. One of the models simulates the spread of DV under three different lockdown scenarios: one long period, two and three shorter intervals that comprise the same interval of time since onset of the Pandemic. Another model studies the interaction between COVID-19 and DV during confinement in relation to the length of the lockdowns. Our findings indicate multiple lockdowns are safer for DV but not necessarily for controlling spread of COVID-19. We also present a derivation of the basic reproduction number for the model involving the interaction between COVID-19 and DV.

Keywords: COVID-19; compartmental models; mathematical biology; domestic violence

1. Introduction

Over the last several months there have been a variety of mathematical models proposed to understand the dynamics of COVID-19 [1–4].These models have helped to provide insight into quantifying the spread, analyzing effective control strategies and developing measures to prevent the spread. Most of these were modeled as compartmental models that were variations of SEIR models [5–7]. While some of them involved expanding the number of compartments needed to represent the models better, others studied the influence of control strategies used in these models such as the influence of face

masks or lockdown strategies to gain more insights. Some of these interventions opened up other challenges.

Lockdowns and confinement strategies have been implemented worldwide as a common attempt of countries to save lives and mitigate the spread of COVID-19. Governments had to weather the storm, with its multiple unfortunate consequences that affect not only the the economy, education and health, but also the basic blocks of society: homes. Pandemic-related fear, health worries, financial stress and isolation during lockdown all take a toll on mental health that affects peace at home. In consequence, if the home is susceptible to DV, confinement under this deteriorating mental health climate and abnormally high interaction at home is well described as a perfect storm of DV, in particular Intimate Partner Violence (IPV) [8, 9].

Since 2010 the CDC report on Intimate Partner Violence (IPV) [10] finds that this is a significant public health problem in the US with long-term health consequences and negative impacts. The CDC fact sheets defines IPV as "Physical violence, sexual violence, stalking, psychological aggression, or control of reproductive or sexual health by a current or former intimate partner." It acknowledges that DV impacts every community and affects all genders, ages and sexual orientations. The 2010–2012 state report data describes IPV as common. In their lifetimes 25% of women, and 10% of men have experienced stalking, physical or sexual violence by an Intimate Partner, according to the National Data on Intimate Partner Violence, Sexual Violence, and Stalking. In addition, US crime reports suggests that around half of all female homicides are committed by former or current male intimate partner. Unfortunately, the latest CDC National Intimate Partner and Sexual Violence Survey (NISVS) published data access is for year 2015, and the National Violent Death Reporting System up to 2016.

In this work a population dynamics model of DV is considered. According to the Exposure Reduction Theory [11], lockdown will amplify the opportunity for abusers to interact with victims in unsafe homes. This social problem is notoriously under-reported as even the definition of "violence" is dependent on the individual's perception. Victims of DV are reluctant to denounce their abusers, and even deny their condition particularly in cultures that condone the use of violence in intimate relations. Furthermore, during lockdown, calls to DV helpline and police reports have shown a counter-intuitive decrease attributed to communication and mobility restrictions, reduced availability of help services and the increased sense of control of the abuser over the victim [12] that may decrease violent incidents triggered by dominance struggles. Some efforts to measure the problem include studying the severity of DV-associated trauma [13], statistical studies of government data, and conducting phone interviews [14]. Nonetheless, data from police reports, calls to helplines, interviews and injury data are important to measure a rise in the violence index [15], but limited in order to account for the number of Victims of DV during the Lockdown.

The outline of this work is as follows. In section 2, we introduce a baseline COVID-19 model that was introduced in [3] which included a confinement compartment. We will introduce two new models that will incorporate DV. Model 1 will include a new DV model combined with baseline COVID-19 model without the spread of COVID-19 inside the confinement. In Model 2, we will include both COVID-19 dynamics along with compartments for DV victims that get infected as well. The goal for introducing Model 1 is to investigate the hypothesis on DV as the number of lockdowns increase in the absence of COVID-19 dynamics within the confinement compartment. An initial definition of DV that uses both Victims and Abusers will help study the impact of the multiple lockdown strategies on multiple victims per abuser. This behaviour of increased abuse over longer periods of confinement is

well documented in the media. In Model 2 we note that, as the pandemic spreads, there are Infected individuals in confinement, and therefore we have a double epidemic (COVID-19 coupled with DV) inside confinement. To study the dynamic of both epidemics we simplify the first model to study victims only of DV that can also be infected by COVID-19. In this model the progression of the coupled epidemics of DV and COVID-19 is studied during one extensive lockdown period. This warrants the assumption of a completely susceptible population in a wider definition of DV, as the long period of confinement is assumed to be more disruptive to social dynamics at home. In section 3, we derive a basic reproduction number for Model 2. The numerical results for the models are shown in Section 4 and models are validated for benchmark examples.

2. Mathematical model and analysis

Over the past few months, many parts of the globe have seen curfews, quarantines, and similar restrictions (described as stay-at-home orders, shelter-in-place orders, shutdowns, or lockdowns). A Free-Lockdown Hybrid approach was developed by Mellone et. al in [16] to model lockdown and a free phase. In [3] a mathematical model of COVID-19 with an explicit confinement compartment has been introduced into a deterministic COVID-19 Model 0 as illustrated in Figure 1. In this work we will further develop both strategies adding multiple lockdowns and the spread of DV during confinement.

The equations derived from the flow diagram of the original Model 0 are included in (2.1). Parameters are described in Table 1.

Table 1. Definition of Parameters in the Baseline COVID-19 model.

Parameter	Definition
β	Transmission Rate
σ	Rate at which Exposed individuals become Infected
ω	Rate at which Asymptomatic individuals become Recovered
ξ	Rate at which Symptomatic individuals become Quarantined or Isolated
γ	Rate at which Quarantined individuals become Hospitalized or Recovered
$1/\alpha^R$	Duration at which Hospitalized individuals who recover remain hospitalized
$1/\alpha^D$	Duration at which Hospitalized individuals who die remain hospitalized
x	Rate at which Hospitalized individuals die
$\hat{x}$	Mortality Rate of Hospitalized individuals with access to an ICU Bed
p	Fraction of Symptomatic individuals out of Exposed individuals
q	Fraction of Hospitalized individuals out of Quarantined individuals

In this model, an extended SEIR mathematical model was considered as shown in figure 1 that incorporates multiple classes of infections in humans, where susceptible individuals (S) become exposed (E) and may either become asymptomatic (I^A) and symptomatic (I^S). These were assumed to be equally infectious and of similar duration (period of infectiousness) as well as quarantine (Q), recovered (R), hospitalized (H) and dead (D) sub-populations. Following the subgroup compartments presented in [17], I^A progress to R, and are not to be associated with pre-symptomatic individuals that are included in compartment E. Our model further assumes that all I^S progress to Q at a ξ rate before progressing to either H or R compartments. The governing differential equations are given as
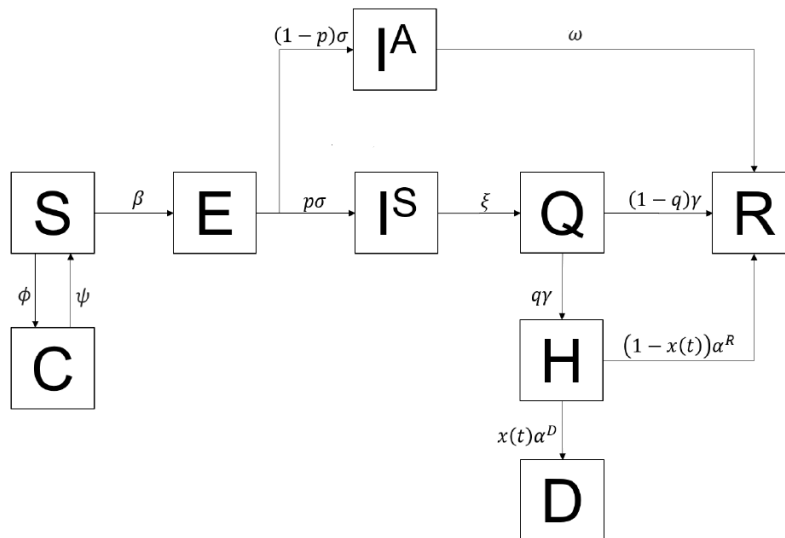
Figure 1. Model 0 Flow Diagram of an Explicit COVID-19 Model.

follows with prescribed parameters including rates for transmission, exposure, infection, quarantine and hospitalization as given in Table 1.

$$
\begin{aligned}
\dot{S}(t) &= -\phi S + \psi S - \beta S \left(\frac{I^A + I^S}{N} \right) \\
\dot{C}(t) &= \phi S - \psi S \\
\dot{E}(t) &= \beta S \left(\frac{I^A + I^S}{N} \right) - \sigma E \\
\dot{I^A}(t) &= (1 - p)\sigma E - \omega I^A \\
\dot{I^S}(t) &= p\sigma E - \xi I^S \\
\dot{H}(t) &= q\gamma Q - ((1 - x)\alpha^R + x\alpha^D)H \\
\dot{Q}(t) &= \xi I^S - \gamma Q \\
\dot{R}(t) &= \omega I^A + (1 - \xi)I^S + (1 - q)\gamma Q + (1 - x)\alpha^R H \\
\dot{D}(t) &= x\alpha^D H
\end{aligned}
\tag{2.1}
$$

In this model susceptible individuals S were assumed to become confined at a rate of ϕ and confined individuals become susceptible at the lift of a lockdown with a rate of ψ. Here ϕ and ψ are defined as Dirac Delta functions based on lockdown times:

$$
\begin{aligned}
\phi(t) &= A\delta(t - tlock) \\
\psi(t) &= B\delta(t - tlift)
\end{aligned}
$$

where A is the fraction of susceptible individuals that enter confinement, B is the fraction of confined individuals that become susceptible, $tlock$ is the lockdown time in days, and $tlift$ is the lockdown lift time in days since epidemic onset.

Next we will expand on this work to develop multiple models that will help to provide insights with respect to lockdown strategies through such confinement approaches in homes susceptible to DV.

2.1. Model 1: a coupled lockdown and DV model

In this section DV incidence during lockdown is added to the COVID-19 Model 0. This preliminary model assumes that only the Susceptible individuals S go into confinement, and that only a fraction of these individuals are susceptible to DV, as is the case with IPV. Model 1 accounts for Victims and Abusers in confinement that are COVID-19 free and in households susceptible to DV. Model 1 assumes that the duration of lockdown will increase DV incidents.

The Confinement compartment C from Model 0 is expanded to Figure 2. DV is modeled using dynamics similar to SIR with compartments for: individuals in safe homes not susceptible to DV (S_1), individuals susceptible to DV (S_2), Victims (V), Abusers (A) and Removed (R) variables. The R^C represents people that have been removed permanently from the unsafe home that include incarceration or restraining orders. All other DV variables (S_1, S_2, A, V) are individuals who have not been exposed/infected with COVID-19, confined to the home by Lockdown orders imposed by the government, and return to the COVID-19 dynamics at the lift of the lockdown period. Specifically, we will assume that confinement removes a fraction of the susceptible (S) population at a rate given by $\rho\phi = \rho\phi(t)$. DV shows logistic growth within confinement because of increased stress, alcohol consumption at home and amplified exposure [11]. The corresponding model equations 2.2 enhanced using additional DV states as described in 2.3–2.7.
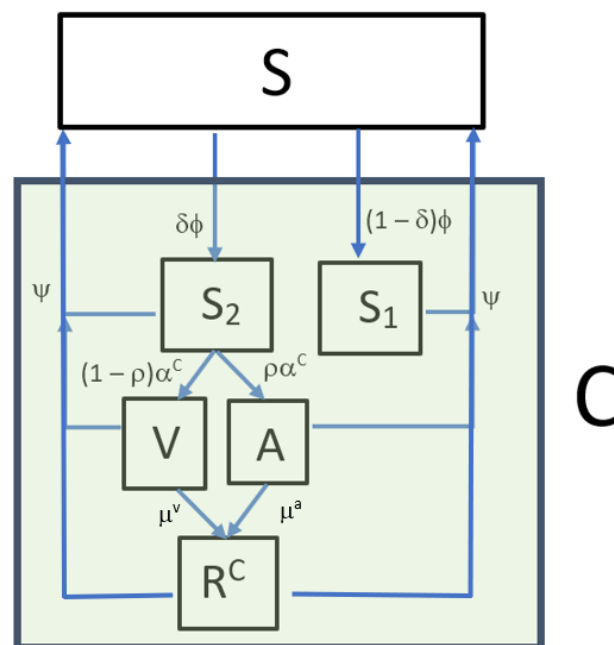
Figure 2. Model 1 flow diagram of Model 1 DV-confinement compartment.

The parameters for the DV component of the model are described in Table 2. Furthermore in Table 3 the initialization for the model implementation and references of the parameters are included.

Table 2. DV parameters.

Parameter	Description
δ	Proportion of Susceptible in unsafe homes
ρ	Proportion of Abusers in DV incident
$\alpha^C(t)$	Time dependent DV index
α^V	DV index
β^C	transmission rate in confinement
μ^V	Separation via protection parameter of victims
μ^A	Removal parameter of abusers due to separation
m	Proportion of victims that escape DV cycle
K	Maximum number of individuals in DV susceptible households
N, N^C	Total population and confined population respectively

Table 3. Initialization and references.

Parameter Initialization	Reference
$\rho = 0.25$	[18]
$\alpha^C(t) = 0.015 + 0.025t$, per month	[19] and [15]
$\mu^V = 0.001$	[20]
$\mu^A \in [0.01, 0.2]$ per 100,000	[21]
K = 410,700	[18]
N= 3,285,874	PR Census, April 1, 2020
$m = 0.01$	assumed
$\delta = 0.25$	assumed
$\mu_D = 0.000005$	assumed
$\beta^C = 0.4$	assumed
$\gamma^C = 1/10$	assumed
$\sigma^C = 1/6$	assumed

$$
\begin{aligned}
\dot{S}(t) &= -\phi S + \psi(S_1 + S_2 + A + V + R^C) - \beta S \left(\frac{I^A + I^S}{N} \right) \\
\dot{E}(t) &= \beta S \left(\frac{I^A + I^S}{N} \right) - \sigma E \\
\dot{I}^A(t) &= (1 - p)\sigma E - \omega I^A \\
\dot{I}^S(t) &= p\sigma E - \xi I^S \\
\dot{H}(t) &= q\gamma Q - ((1 - x)\alpha^R + x\alpha^D)H \\
\dot{Q}(t) &= \xi I^S - \gamma Q \\
\dot{R}(t) &= \omega I^A + (1 - q)\gamma Q + (1 - x)\alpha^R H \\
\dot{D}(t) &= x\alpha^D H
\end{aligned}
\tag{2.2}
$$

$$\dot{S}_1(t) = (1 - \delta)\phi S - \psi S_1 \tag{2.3}$$

$$\dot{S}_2(t) = \delta\phi S - \alpha^c S_2 \left(1 - \frac{S_2}{K}\right) - \psi S_2 \tag{2.4}$$

$$\dot{A}(t) = \rho\alpha^c S_2 \left(1 - \frac{S_2}{K}\right) - \mu^A A - \psi A \tag{2.5}$$

$$\dot{V}(t) = (1 - \rho)\alpha^c S_2 \left(1 - \frac{S_2}{K}\right) - \mu^v V - \psi V \tag{2.6}$$

$$\dot{R}^C(t) = \mu^a A + \mu^v V - \psi R^C \tag{2.7}$$

Theorem 2.1. *All the solutions of the DV model structure that initiate in $\mathbb{R}^4_+$ are bounded inside the region defined by* $\left\{ (S_1, S_2, A, V) \in \mathbb{R}^4 : 0 \le S_1 + S_2 + A + V \le \dfrac{\phi S}{\psi} \right\}_{t \to \infty}$

Proof. One may note that adding Eqs (2.3)–(2.7), we get,

$$\begin{aligned}
\dot{S}_1(t) + \dot{S}_2(t) + \dot{A}(t) + \dot{V}(t) &= \phi S - \psi(S_1 + S_2 + A + V) - \mu^A A - \mu^V V \\
&\le \phi S - \psi(S_1 + S_2 + A + V)
\end{aligned}$$

yielding

$$\frac{d}{dt}(S_1 + S_2 + A + V) + \psi(S_1 + S_2 + A + V) \le \phi S$$

Then, we have

$$S_1 + S_2 + A + V \le \left(S_1(0) + S_2(0) + A(0) + V(0) - \frac{\phi S}{\psi} \right) e^{-\psi t} + \frac{\phi S}{\psi}$$

Hence as $t \to \infty$ we get the solution $(S_1, S_2, A, V) \subset \left[0, \dfrac{\phi S}{\psi} \right]$. $\qquad\square$

In the next section we introduce a model with two epidemics: DV and COVID-19 within the confinement.

2.2. *Model 2: lockdown, COVID-19 and DV*

Multiple lockdowns have the additional risk of having and increased number of exposed or infected individuals in a given home as the disease continues to spread. It is common to have a family member, particularly asymptomatic, that will infect others in the household. In order to develop a Model 2 with COVID-19 and DV dynamics we will first focus only in the Confinement dynamics during Lockdown. Model 2 assumptions follow.

- DV dynamics will be simplified to the Victim variable V only, that may be also affected by COVID-19.
- At initialization there is No DV Victims in the Lockdown confinement.
- Quarantine Q is not applicable in the confinement.
- All the population in confinement are susceptible to some form of DV as perceived by the victims.
- The COVID-19 confinement variables will be initialized at lockdown as 80 % of its corresponding pre-confinement values.

- I^S, I^A are generalized into an infected compartment I.
- In confinement C, COVID-19 is much slower to propagate limited to the number of people in a household with an Exposed or Infected member [22].
- D^C and V_D accounts for COVID-19 and DV deceased during Lockdown.
- Infected individuals I, V_I are hospitalized during lockdown with a common parameter.
- A fraction m of victims of DV can escape the violence cycle with the help of programs, friends and family.

The new governing equations in (2.8) follow the modified Confinement/Lockdown dynamics illustrated in Figure 3.

$$
\begin{aligned}
\dot{S^C}(t) &= mV_S - \beta^C S^C \left(\frac{I^C + V_I}{N^C} \right) - \alpha^V S^C \\
\dot{E^C}(t) &= mV_E + \beta^C S^C \left(\frac{I^C + V_I}{N^C} \right) - \alpha^V E^C - \sigma^C E^C \\
\dot{I^C}(t) &= mV_I - \alpha^V I^C - \gamma^C I^C + \sigma^C E^C \\
\dot{R^C}(t) &= mV_R + (1 - q)\gamma^C I^C - \alpha^V R^C + (1 - x)\alpha^R H \\
\dot{H^C}(t) &= q\gamma^C (I^C + V_I) - ((1 - x)\alpha^R + x\alpha^D) H^C \\
\dot{D^C}(t) &= x\alpha^D H^C \\
\dot{V_S}(t) &= -(\mu_D + m)V_S - \beta^C V_S \left(\frac{I^C + V_I}{N^C} \right) + \alpha^V S^C \\
\dot{V_E}(t) &= -(\mu_D + m)V_E + \beta^C V_S \left(\frac{I^C + V_I}{N^C} \right) + \alpha^V E^C - \sigma^C V_E \\
\dot{V_I}(t) &= -(\mu_D + m)V_I + \alpha^V I^C - \gamma^C V_I + \sigma^C V_E \\
\dot{V_R}(t) &= -(\mu_D + m)V_R + \alpha^V R^C + (1 - q)\gamma^C V_I \\
\dot{V_D}(t) &= \mu_D(V_S + V_E + V_I + V_R)
\end{aligned}
\tag{2.8}
$$

3. Analysis

In this section, we will derive a basic reproduction number $\mathcal{R}_0$ that can be used to measure the transmission potential of COVID-19 as proposed by the system (2.8). $\mathcal{R}_0$ is the average number of secondary infections produced by a typical case of an infection in a population where everyone is susceptible [23].

Let us recall that the proposed mathematical model for COVID-19 includes sub-populations with different infectious states. Therefore, we will employ a general approach called the *Next Generation Matrix* [24] to find the basic reproduction number $\mathcal{R}_0$ which is given by the following theorem.

Theorem 3.1. *The basic reproduction number $\mathcal{R}_0$ is given by*

$$
\mathcal{R}_0 = \frac{R}{2} \pm \frac{\sqrt{R^2 + 4\left(R_1^a R_1^b - R_2^a R_2^b\right)}}{2}
$$
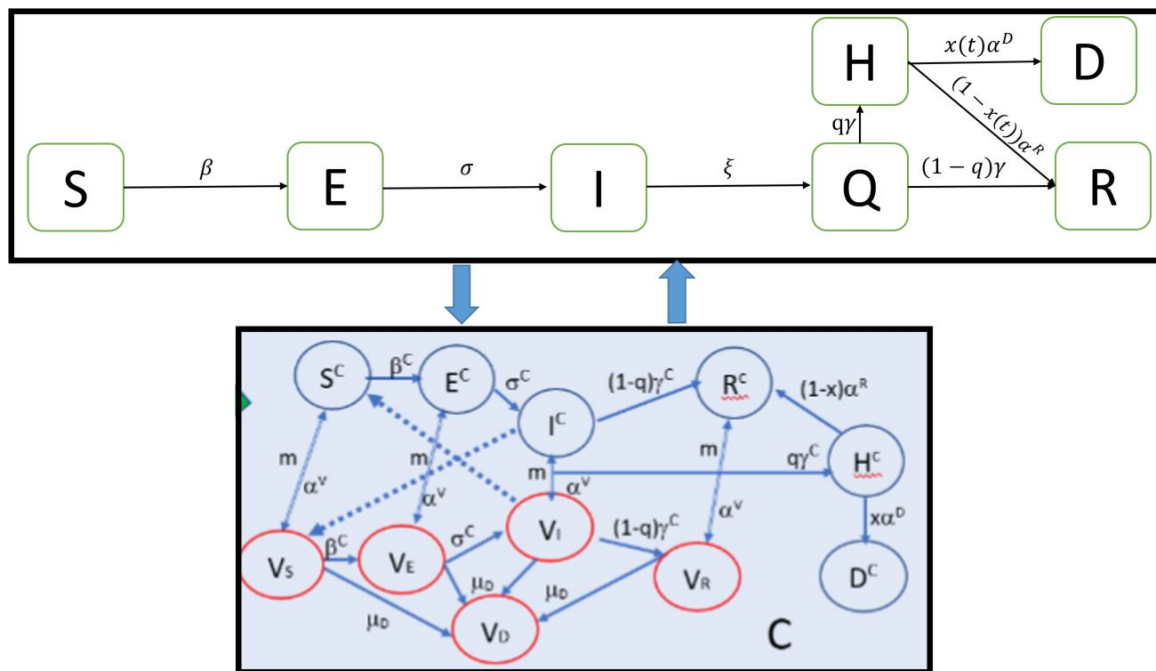
Figure 3. Lockdown Flow Diagram of COVID-19 and DV: Switch between simplified Model 0 (Top panel) and System (2.8) in Lockdown (Bottom).

where,

$$R = \frac{\beta^C \frac{S^C}{N^C}\left(\mu_D + m + \gamma^C + \alpha^V\right)\sigma^C}{(\alpha^V + \sigma^C)[(\alpha^V + \gamma^C)(\mu_D + m + \gamma^C) - m\alpha^V]} + \frac{\beta^C \frac{V_S}{N^C}\left(m + \gamma^C + \alpha^V\right)\sigma^C}{(\mu_D + m + \sigma^C)[(\alpha^V + \gamma^C)(\mu_D + m + \gamma^C) - m\alpha^V]}$$

$$R_1^a = \frac{\beta^C \frac{V_S}{N^C}(\mu_D + m + \gamma^C + \alpha^V)\sigma^C + \alpha^V[(\alpha^V + \gamma^C)(\mu_D + m + \gamma^C) - m\alpha^V]}{(\alpha^V + \sigma^C)[(\alpha^V + \gamma^C)(\mu_D + m + \gamma^C) - m\alpha^V]}$$

$$R_1^b = \frac{\beta^C \frac{S^C}{N^C}(m + \gamma^C + \alpha^V)\sigma^C + m[(\alpha^v + \gamma^C)(\mu_D + m + \gamma^C) - m\alpha^V]}{(\mu_D + m + \sigma^C)[(\alpha^V + \gamma^C)(\mu_D + m + \gamma^C) - m\alpha^V]}$$

$$R_2^a = \frac{\beta^C \frac{S^C}{N^C}(\mu_D + m + \gamma^C + \alpha^V)\sigma^C}{(\alpha^V + \sigma^C)[(\alpha^V + \gamma^C)(\mu_D + m + \gamma^C) - m\alpha^V]}$$

$$R_2^b = \frac{\beta^C \frac{V_S}{N^C}(m + \gamma^C + \alpha^V)\sigma^C}{(\mu_D + m + \sigma^C)[(\alpha^V + \gamma^C)(\mu_D + m + \gamma^C) - m\alpha^V]}$$

Proof. Given that the infectious states: E^C, I^C, V_E, V_I in system (2.8) we can create a vector $\mathcal{F}$ that represents the new infections flowing only into the exposed compartments given by:

$$\mathcal{F} = \left\{ mV_E + \beta^C \frac{S^C}{N^C}(I^C + V_I), \; 0, \beta^C \frac{V_S}{N^C}(I^C + V_I) + \alpha^V E^C, 0 \right\} \tag{3.1}$$

Along with $\mathcal{F}$, we will also consider $\mathcal{V}$ which denotes the outflow from the infectious compartments in system (2.8) which is given by:

$$\mathcal{V} = \left\{ (\alpha^V + \sigma^C)E^C, \; -mV_I + (\alpha^V + \gamma^C)I^C - \sigma^C E^C, \; (\mu_D + m + \sigma^C)V_E, \; (\mu_D + m + \gamma^C)V_I - \alpha^V I^C - \sigma^C V_E \right\} \tag{3.2}$$

Next, we compute the Jacobian F from $\mathcal{F}$ given by,

$$F = \begin{pmatrix} 0 & \beta^C \dfrac{S^C}{N^C} & m & \beta^C \dfrac{S^C}{N^C} \\[2mm] 0 & 0 & 0 & 0 \\[2mm] \alpha^V & \beta^C \dfrac{V_S}{N^C} & 0 & \beta^C \dfrac{V_S}{N^C} \\[2mm] 0 & 0 & 0 & 0 \end{pmatrix}$$

and the Jacobian V from $\mathcal{V}$ given by,

$$V = \begin{pmatrix} (\alpha^V + \sigma^C) & 0 & 0 & 0 \\[2mm] -\sigma^C & (\alpha^V + \gamma^C) & 0 & -m \\[2mm] 0 & 0 & \mu_D + m + \sigma^C & 0 \\[2mm] 0 & -\alpha^V & -\sigma^C & \mu_D + m + \gamma^C \end{pmatrix}$$

Using these, one can now compute the inverse of the next generation matrix FV^{-1} to be:

$$FV^{-1} = \frac{1}{ch - df} \begin{pmatrix} \dfrac{bp(f - h)}{a} & p(h - f) & \dfrac{bp(d - c) - d(ch - df)}{e} & p(c - d) \\[4mm] 0 & 0 & 0 & 0 \\[4mm] \dfrac{bq(f - h) - f(ch - df)}{a} & q(h - f) & \dfrac{bq(d - c)}{e} & q(c - d) \\[4mm] 0 & 0 & 0 & 0 \end{pmatrix} \tag{3.3}$$

where,

$$
\begin{aligned}
a &= \alpha^V + \sigma^C \\
b &= -\sigma^C \\
c &= \alpha^V + \gamma^C \\
d &= -m \\
e &= \mu_D + m + \sigma^C \\
f &= -\alpha^V \\
g &= -\sigma^C \\
h &= \mu_D + m + \gamma^C \\
p &= \beta^C \frac{S^C}{N^C} \\
q &= \beta^C \frac{V_S}{N^C}
\end{aligned}
$$

Note that (i, j) entry of the Next Generation Matrix FV^{-1} is the expected number of secondary infections in compartment i produced by individuals initially in compartment j assuming that the environment seen by the individual remains homogeneous for the duration of its infection. Also, matrix FV^{-1} is non-negative and therefore has a non-negative eigenvalue. The basic reproduction number can then be computed as $\mathcal{R}_0 = \rho\left(FV^{-1}\right)$ which is the spectral radius of the matrix. This non-negative eigenvalue is associated with a non-negative eigenvector which represents the distribution of infected individuals that produce the greatest number $\mathcal{R}_0$ of secondary infections per generation.

For our system (2.8), the basic reproduction number $\mathcal{R}_0$ corresponds to the dominant eigenvalue of the matrix in Eq (3.3) which can be computed by considering the characteristic equation

$$\det(FV^{-1} - \lambda I) = 0.$$

Note that,

$$
FV^{-1} - \lambda I =
\begin{pmatrix}
\dfrac{bp(f-h)}{a(ch-df)} - \lambda & \dfrac{p(h-f)}{(ch-df)} & \dfrac{bp(d-c)-d(ch-df)}{e(ch-df)} & \frac{p(c-d)}{(ch-df)} \\[3mm]
0 & -\lambda & 0 & 0 \\[3mm]
\dfrac{bq(f-h)-f(ch-df)}{a(ch-df)} & \dfrac{q(h-f)}{(ch-df)} & \dfrac{bq(d-c)}{e(ch-df)} - \lambda & \dfrac{q(c-d)}{(ch-df)} \\[3mm]
0 & 0 & 0 & -\lambda
\end{pmatrix}
\tag{3.4}
$$

Solving for the eigenvalues λ setting the determinant of Eq (3.4) and simplifying, we get,

$$
\mathcal{R}_0 = \frac{R}{2} \pm \frac{\sqrt{R^2 + 4\left(R_1^a R_1^b - R_2^a R_2^b\right)}}{2}
$$

where,

$$R = \frac{\beta^C \frac{S^C}{N^C}\left(\mu_D + m + \gamma^C + \alpha^V\right)\sigma^C}{(\alpha^V + \sigma^C)[(\alpha^V + \gamma^C)(\mu_D + m + \gamma^C) - m\alpha^V]} + \frac{\beta^C \frac{V_S}{N^C}\left(m + \gamma^C + \alpha^V\right)\sigma^C}{(\mu_D + m + \sigma^C)[(\alpha^V + \gamma^C)(\mu_D + m + \gamma^C) - m\alpha^V]}$$

$$R_1^a = \frac{\beta^C \frac{V_S}{N^C}(\mu_D + m + \gamma^C + \alpha^V)\sigma^C + \alpha^V[(\alpha^V + \gamma^C)(\mu_D + m + \gamma^C) - m\alpha^V]}{(\alpha^V + \sigma^C)[(\alpha^V + \gamma^C)(\mu_D + m + \gamma^C) - m\alpha^V]}$$

$$R_1^b = \frac{\beta^C \frac{S^C}{N^C}(m + \gamma^C + \alpha^V)\sigma^C + m[(\alpha^v + \gamma^C)(\mu_D + m + \gamma^C) - m\alpha^V]}{(\mu_D + m + \sigma^C)[(\alpha^V + \gamma^C)(\mu_D + m + \gamma^C) - m\alpha^V]}$$

$$R_2^a = \frac{\beta^C \frac{S^C}{N^C}(\mu_D + m + \gamma^C + \alpha^V)\sigma^C}{(\alpha^V + \sigma^C)[(\alpha^V + \gamma^C)(\mu_D + m + \gamma^C) - m\alpha^V]}$$

$$R_2^b = \frac{\beta^C \frac{V_S}{N^C}(m + \gamma^C + \alpha^V)\sigma^C}{(\mu_D + m + \sigma^C)[(\alpha^V + \gamma^C)(\mu_D + m + \gamma^C) - m\alpha^V]}$$

$\square$

Note that Theorem 3.1 yields a general result for the basic reproduction number $\mathcal{R}_0$ corresponding to the COVID-19 disease transmission model given by system (2.8).

Remark 3.2. If $m = 0$ and $\mu_D = 0$ then we have, $\mathcal{R}_0 = \frac{R}{2} \pm \frac{\sqrt{R^2 + 4\left(R_1^a R_1^b - R_2^a R_2^b\right)}}{2}$ where,

$$R = \frac{\beta^C}{\gamma^C} \frac{\sigma^C}{\alpha^V + \sigma^C} \frac{S^C}{N^C} + \frac{\beta^C}{\gamma^C} \frac{V_S}{N^C}$$

$$R_1^a = \frac{\beta^C}{\gamma^C} \frac{\sigma^C}{\alpha^V + \sigma^C} \frac{V_S}{N^C} + \frac{\alpha^V}{(\alpha^V + \sigma^C)}$$

$$R_1^b = \frac{\beta^C}{\gamma^C} \frac{S^C}{N^C}$$

$$R_2^a = \frac{\beta^C}{\gamma^C} \frac{\sigma^C}{\alpha^V + \sigma^C} \frac{S^C}{N^C}$$

$$R_2^b = \frac{\beta^C}{\gamma^C} \frac{V_S}{N^C}$$

Remark 3.3. If $m = 0$, $\mu_D = 0$ and $\alpha^V = 0$ then we have,

$$\mathcal{R}_0 = \frac{\beta^C}{\gamma^C} \frac{(S^C + V_S)}{N^C}$$

showing the expected definition of a basic reproduction number to be the ratio of the transmission rate to the recovery rate when $S^C + V_S \approx N^C$.

Table 4. Simulation results for Model 1.

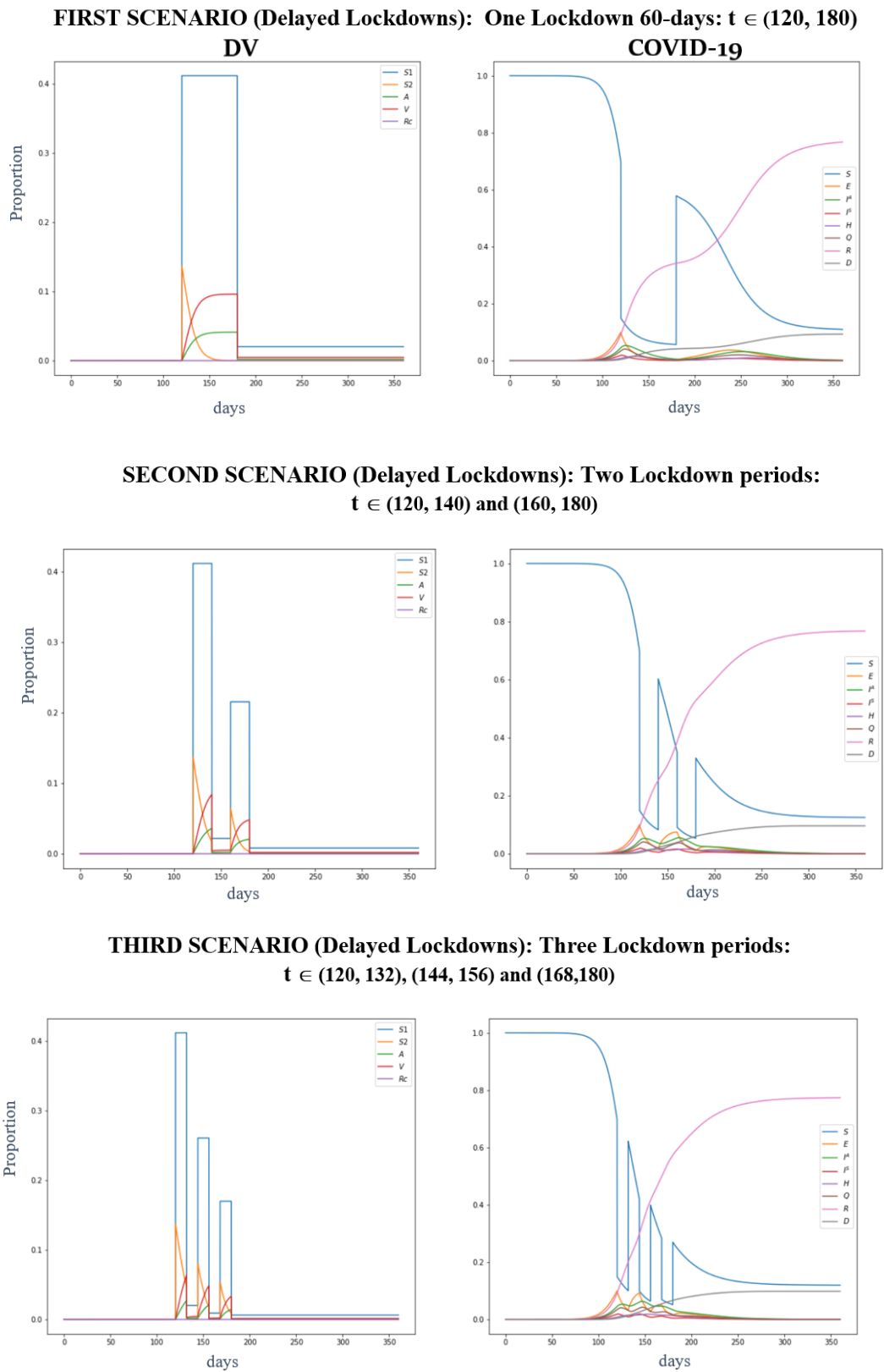| Lockdown Scenario (Population N = 3.3 million)	COVID-19 Max Infection	DV Max Abusers	DV Max Victims
First Scenario: One Lockdown (120, 180) days	2.28 e05	1.35 e05	3.14 e05
Second Scenario: Two Lockdowns (120,140) and (160,180) days	2.33 e05	1.18 e05	2.76 e05
Third Scenario: Three Lockdowns (120,132), (144,156), and (168,180) days	2.68 e05	0.89 e05	2.09 e05

4. Computational results

In this section, we conduct simulations for the new models, namely Model 1 given by system (2.2)-(2.7) and Model 2 given by system (2.8) introduced in the paper.

Model 1 simulations were obtained for three Lockdown scenarios of 80% confinement. The three scenarios correspond to one, two and three lockdowns of varying duration that comprise the same delayed period: days 120 to 180 from onset. This period was selected because in the baseline Model 0 [3] simulation it was associated with the peak number of infected I^S . The three scenarios were designed as follows:
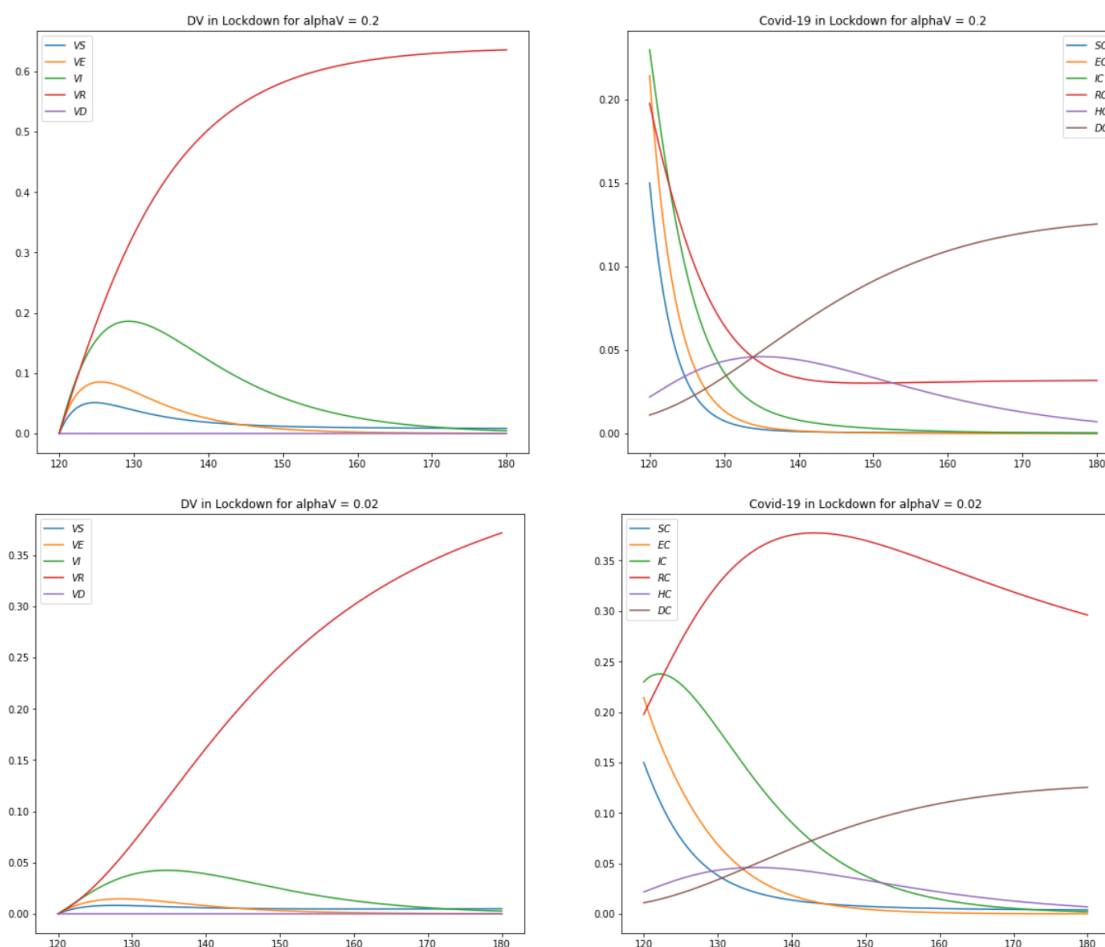
- one 60-days lockdown
- two 20-day lockdowns separated by a 10-days lift, and
- three 12-days lockdowns separated by 12-days lifts

Results in Figure 4 show the shifts from lockdown to lift periods for the DV problem in compartment C and the COVID-19 dynamics outside. Figure 4 graphs shows the coupling in time of the multiple lockdowns and lifts that confine 80% of the population. On the left side the DV graphs show and increase of violence illustrated with a sharp reduction in violence-susceptible homes S_2 compared to the constant population in safe homes S_1 during confinement. On the right, the COVID-19 graphs show a dramatic reduction of all variables in First Scenario, one long lockdown, compared to the other scenarios. This is well illustrated in the shape of the increasing R Curve that show multiple inflections in the First Scenario corresponding to reductions in the infection rates. Multiple waves of the I curve and closer peaks of infection can also be observed from First to the Third scenario. Nonetheless, the Third Scenario with three short lockdowns give a better outlook for DV with reduced victims V and abusers A compared to the worst case First Scenario. The numbers in Table 4 show that COVID-19 Maximum Infection and Death, in the blue columns, are going up while the corresponding DV numbers are decreasing in our simulation as the number of lockdowns increase in a time interval: 120 to 180 days since epidemic onset. Each row corresponds to the three scenarios in Figure 4.

A limitations of Models 0 and 1 is the dependence on the switch functions $\phi(t), \psi(t)$ that have been conveniently programmed to identify the lockdown date and initialize the confinement variables. Results were obtained using the python Runge-Kutta 45 (RK45) solver, showing another success of

FIRST SCENARIO (Delayed Lockdowns): One Lockdown 60-days: t ∈ (120, 180)

DV COVID-19

SECOND SCENARIO (Delayed Lockdowns): Two Lockdown periods:
t ∈ (120, 140) and (160, 180)

THIRD SCENARIO (Delayed Lockdowns): Three Lockdown periods:
**t ∈ (120, 132), (144, 156) and (168,180)**

Figure 4. Model 1 simulation results as in Table 4.

Figure 5. Model 2 Results for high and low α^V.

the Dormand-Prince algorithm [25]. For the more complex Models 2 we have further developed the switch functions into hybrid lockdown by initializing when the variables according at lockdown and lift, similar to [16].

Simulations for Model 2 were obtained in Figure 5 illustrating the dynamics in confinement when COVID-19 and DV are present. This figure show a high sensitivity of the variables to the DV parameter α^V that models the violence index increase during the pandemic reported in various countries. Therefore, we conducted Model 2 simulations modifying the violence-index parameter $\alpha^V \in [0, 1]$. For each run we compute the maximum value of the infectious variables for COVID-19 (E^C, I^C) and for the DV-victims that have been affected by COVID-19 (V_E, V_I). In Figure 6 we see two graphs that correspond to a long and short lockdown periods. It can be readily seen that an increase in violence α^V will not change the maximum values of variables E^C, I^C, because both variables continue to rapidly decrease from its largest initial values. On the other hand, the graphs show a dramatic increase in the maximum values of infectious states that correspond to DV V_E, V_I.

From our theoretical results in Theorem 3.1, we computed the $\mathcal{R}_0$ as a function of α^V, β^C and generated Figure 7 for our simulation parameters. We can see that the highest $\mathcal{R}_0$ occur when β^C is closer to 1. When α^V increases the $\mathcal{R}_0$ decreases.
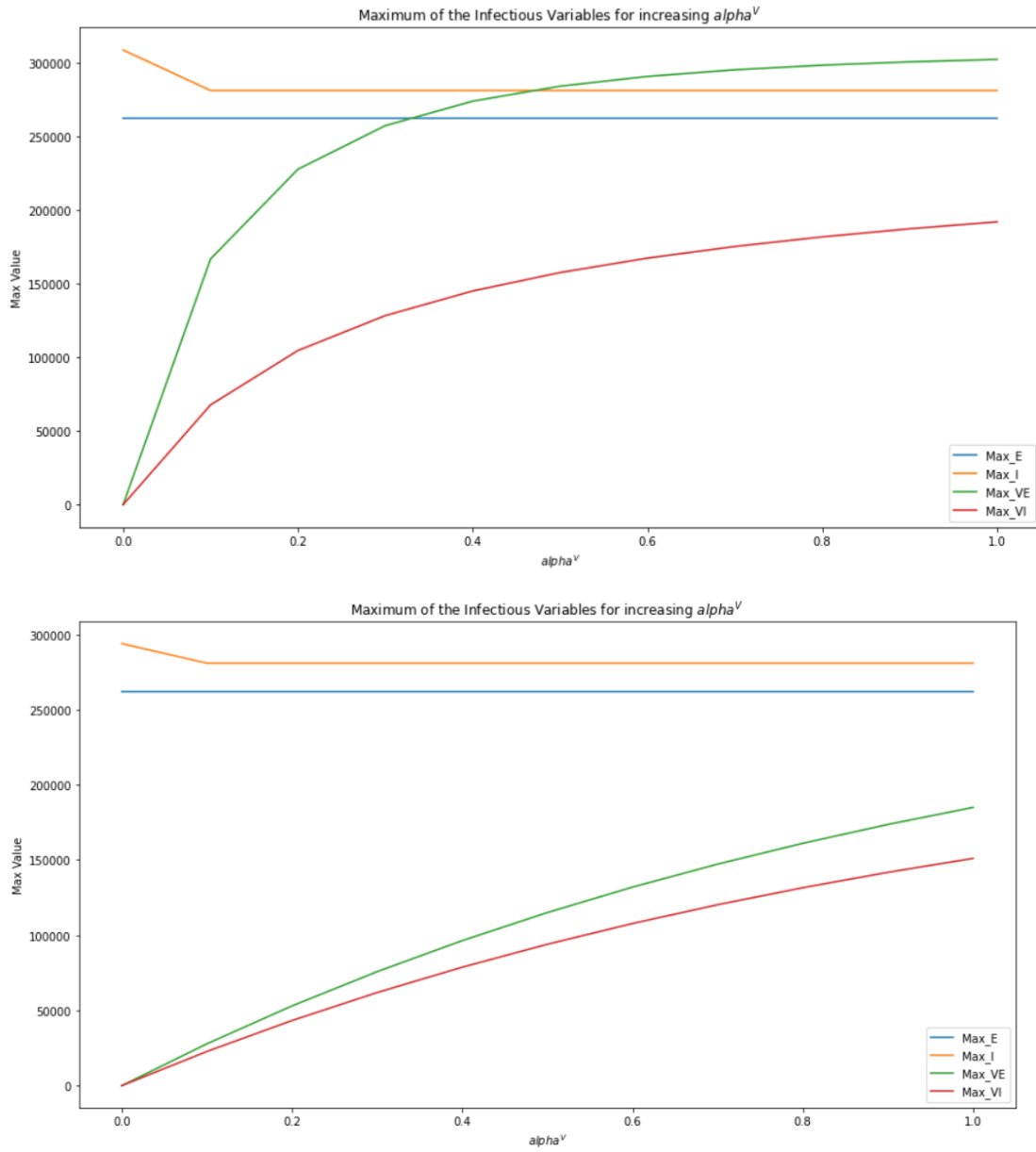
Figure 6. Max of Infectious states vs. α^V for long (top) and short (bottom) lockdowns.

$$R_0(\alpha^V, \beta^C)$$
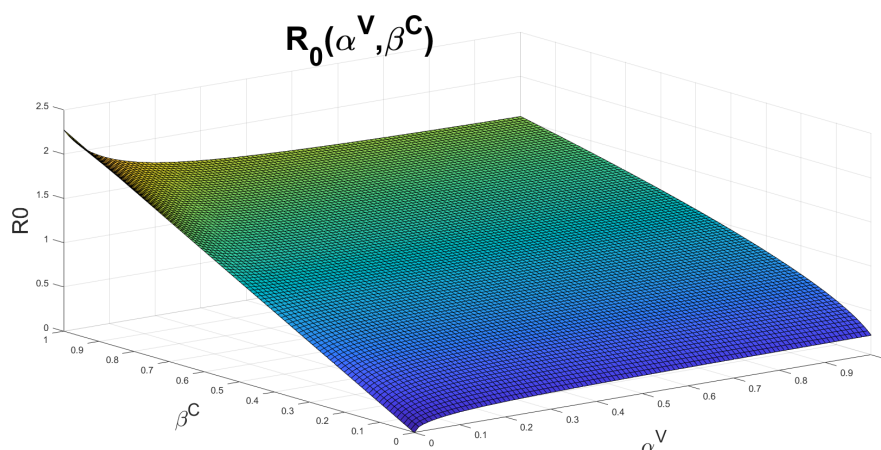
Figure 7. $\mathcal{R}_0$ as a function of DV index α^V and transmission rates β^C.

5. Conclusions

In this work we have developed models and tools that will help study the relationship between lockdowns, the spread of COVID-19 and DV in the hope of mitigating the social problems that follow such drastic measures. Two different models, in increasing level of complexity have been used to simulate the effect of the lockdown strategy in the spread of COVID-19 and DV. Model 1 models the spread of DV under three different lockdown scenarios: one long period, two and three shorter intervals that comprise the same interval of time since onset of the Pandemic. Although a prolonged lockdown will most likely help reduce the spread of COVID-19, it also sends individuals to confinement in an unsafe home when DV is present. Simulations suggest that multiple lockdowns reduce the spread of DV, but one longer lockdown has greater impact in reducing COVID-19. In Model 2 the presence of COVID-19 in homes that are susceptible to DV is simulated. The parameter α^V has been modified to compare the influence on infectious states showing a drastic decrease in the COVID-19 infections and increase in DV victims that are infected. For this complex Model we obtained the $\mathcal{R}_0$ of the model, our main theoretical result.

DV is a problem that affects generations and one worthy of further studies. We hope to continue to develop new models that are data-driven and obtain parameters that are tuned to a particular place and culture. Mathematical modeling tools and methods are of special help in order to compare the effect of lockdown and confinement strategies on the well-being of our society.

While the new models proposed in this work provides great insight into what happens during confinement in terms of the spread of COVID-19 as well as propagation of DV, there is a great need to collect data that can help validate the model parameters, especially, α^V. Along with this one could possibly investigate optimal control strategies through the parameter m that can help break the DV cycle. These two aspects will be considered in forthcoming papers.

Acknowledgments

Conflict of interest

The authors declare there is no conflicts of interest.

References

1. F. Bai, F. Brauer, The effect of face mask use on COVID-19 models, *Epidemiologia*, **2** (2021), 75–83. https://doi.org/10.3390/epidemiologia2010007

2. S. He, Y. Peng, K. Sun SEIR modeling of the COVID-19 and its dynamics, *Nonlinear Dyn.*, **101** (2020), 1667–1680. https://doi.org/10.1007/s11071-020-05743-y

3. C. Ohajunwa, K. Kumar, P. Seshaiyer Mathematical modeling, analysis, and simulation of the COVID-19 pandemic with explicit and implicit behavioral changes, *Comput. Math. Biophys.*, **8** (2020), 216–232. https://doi.org/10.1515/cmb-2020-0113

4. J. Rebaza, On a model of COVID-19 dynamics, *Electron. Res. Archive*, **29** (2021), 2129. https://doi.org/10.3934/era.2020108

5. L. López, X. Rodo, A modified SEIR model to predict the COVID-19 outbreak in Spain and Italy: simulating control scenarios and multi-scale epidemics, *Results Phys.*, **21** (2021), 103746. https://doi.org/10.1016/j.rinp.2020.103746

6. D. Dwomoh, S. Iddi, B. Adu, J. M. Aheto, K. M. Sedzro, J. Fobil, et al., A modified SEIR model to predict the COVID-19 outbreak in Spain and Italy: simulating control scenarios and multi-scale epidemics, *Infect. Dis. Model.*, **6** (2021), 381–397.

7. C. Ohajunwa, P. Seshaiyer, Mathematical modeling, analysis, and simulation of the COVID-19 pandemic with behavioral patterns and group mixing, *Spora: A J. Biomath.*, **7** (2021), 46–60.

8. S. Davidge, A perfect storm: the impact of the COVID-19 pandemic on domestic abuse survivors and the services supporting them, *Bristol: Women's Aid*, **7** (2020), 46–60.

9. K. Usher, N. Bhullar, J. Durkin, N. Gyamfi, D. Jackson, Family violence and COVID-19: Increased vulnerability and reduced options for support, *Int. J. Ment. Health Nurs.*, **29** (2020), 549–552. https://doi.org/10.1111/inm.12735

10. *An Overview of Intimate Partner Violence in the United States — 2010 Findings*, The National Intimate Partner and Sexual Violence Survey, National Center of Injury Prevention and Control, CDC, 2010. Available from: `https://www.cdc.gov/violenceprevention/pdf/nisvs_sofindings.pdf`.

11. L. Dugan, D. Nagin, R. Rosenfeld, Exposure Reduction or Retaliation? The Effects of Domestic Violence Resources on Intimate-Partner Homicide, *Law Soc. Rev.*, **37** (2003), 169–198. https://doi.org/10.1111/1540-5893.3701005

12. G. Barbara, F. Facchin, L. Micci, M. Rendiniello, P. Giulini, C. Cattaneo, et al., COVID-19, Lockdown, and Intimate Partner Violence: Some Data from an Italian Service and Suggestions for Future Approaches, *J. Womens Health*, **29** (2020), 1239–1242. https://doi.org/10.1089/jwh.2020.8590

13. P. L. Esteban, J. Q. Coll, M. X. Martínez, J. C. Biayna, L. Delgado-Flores, Has COVID-19 affected the number and severity of visits to a traumatology emergency department?, *Bone Jt. Open*, **1** (2020), 617–620. https://doi.org/10.1302/2633-1462.110.BJO-2020-0120.R1

14. C. Porter, M. Favara, A. Sánchez, D. Scott, The impact of COVID-19 lockdowns on physical domestic violence: Evidence from a list randomization experiment, *SSM - Population Health*, **14** (2021), 100792. https://doi.org/10.1016/j.ssmph.2021.100792

15. L. C. Hsu, A. Henke, COVID-19, staying at home, and domestic violence, *Rev. Econ. Household*, **19** (2021), 145–155. https://doi.org/10.1007/s11150-020-09526-7

16. A. Mellone, Z. Gong, G. Scarciotti, Modelling, prediction and design of COVID-19 lockdowns by stringency and duration, *Sci. Rep.*, **11** (2021), 1–13. https://doi.org/10.1038/s41598-021-95163-8

17. X. Wang, R. Pasco, K. Pierce, Z. Du, S. Fox, L. A. Meyers, *COVID-19 Healthcare Demand Projections: Austin, Texas*, The University of Texas at Austin, 2020.

18. *Social Institutions and Gender Index (SIGI) regional report on Latin American and Caribbean 2020*, Organization for Economic Cooperative and Development (OECD), 2020.

19. EFE News, *Más de 900 incidentes de violencia de género en Puerto Rico durante el COVID-19*, (Spanish) [More than 900 incidents of IPV in Puerto Rico during COVID-19], 2020. Available from: `www.efe.com/efe/usa/puerto-rico/mas-de-900-incidentes-violencia-genero-en-puerto-rico-durante-el-covid-19/50000110-4243778`.

20. A. González-Ramírez, *Más de 900 incidentes de violencia de género en Puerto Rico durante el COVID-19*, Type Investigations, 2020. Available from: `www.typeinvestigations.org/investigation/2020/06/30/in-puerto-rico-an-epidemic-of-domestic-violence-hides-in-plain-sight/`.

21. P. Zeppegno, C. Gramaglia, S. di Marco, C. Guerriero, C. Consol, L. Loreti, Intimate partner homicide suicide: a mini-review of the literature (2012-2018), *Curr. Psychiatry Rep.*, **21** (2019), 46–60. https://doi.org/10.1007/s11920-019-0995-2

22. L. Roques, E. K. Klein, J. Papaïx, A. Sar, S. Soubeyrand, Impact of Lockdown on the Epidemic Dynamics of COVID-19 in France, *Front. Med.*, **7** (2020), 274. https://doi.org/10.3389/fmed.2020.00274

23. O. Diekmann, J. A. P. Heesterbeek, J. Metz, *On the definition and the computation of the basic reproduction ratio R 0 in models for infectious diseases in heterogeneous populations*, *J. Math. Biol.*, **23** (1990), 365–382. https://doi.org/10.1007/BF00178324

24. F. Brauer, C. Castillo-Chavez, *Mathematical models in population biology and epidemiology*, Texts in Applied Mathematics (TAM, volume 40), Springer-Verlag, New York, 2001.

25. J. R. Dormand, P. J. Prince, A family of embedded Runge-Kutta formulae, *J. Comput. Appl. Math.*, **6** (1980), 19–26. https://doi.org/10.1016/0771-050X(80)90013-3